

Absorption of solar radiation by the atmosphere as determined using satellite, aircraft, and surface data during the Atmospheric Radiation Measurement Enhanced Shortwave Experiment (ARESE)

Francisco P. J. Valero,¹ Patrick Minnis,² Shelly K. Pope,¹ Anthony Bucholtz,¹ Brett C. Bush,¹ David R. Doelling,³ William L. Smith Jr.,³ and Xiquan Dong³

Abstract. Data sets acquired during the Atmospheric Radiation Measurement Enhanced Shortwave Experiment (ARESE) using simultaneous measurements from five independent platforms (GOES 8 geostationary satellite, ER-2, Egrett and Twin Otter aircraft, and surface) are analyzed and compared. A consistent data set can be built for selected days during ARESE on the basis of the observations from these platforms. The GOES 8 albedos agree with the ER 2, Egrett, and Twin Otter measured instantaneous albedos within 0.013 ± 0.016 , 0.018 ± 0.032 , and 0.006 ± 0.011 , respectively. It is found that for heavy overcast conditions the aircraft measurements yield an absorptance of 0.32 ± 0.03 for the layer between the aircraft (0.5–13 km), while the GOES 8 albedo versus surface transmittance analysis gives an absorptance of 0.33 ± 0.04 for the total atmosphere (surface to top). The absorptance of solar radiation estimated by model calculations for overcast conditions varies between 0.16 and 0.24, depending on the model used and on cloud and aerosol implementation. These results are in general agreement with recent findings for cloudy skies, but here a data set that brings together independent simultaneous observations (satellite, surface, and aircraft) is used. Previous ARESE results are reexamined in light of the new findings, and it is concluded that the overcast absorptance in the $0.224\text{--}0.68 \mu\text{m}$ spectral region ranges between 0.04 ± 0.06 and 0.08 ± 0.06 , depending on the particular case analyzed. No evidence of excess clear-sky absorption beyond model and experimental errors is found.

1. Introduction

Disagreements between radiative transfer models and observations have persisted ever since *Fritz* [1951] suggested that the cloudy atmosphere absorbs more solar radiation than is predicted by theory [e.g., *Stephens and Tsay* 1990]. Recently, and nearly simultaneously, *Cess et al.* [1995], *Ramanathan et al.* [1995], and *Pilewskie and Valero* [1995] reported a level of shortwave cloud absorption beyond the ability of any model to predict with conventional microphysical parameters. These three papers were based on a variety of observational sources, aircraft, surface, and satellite, and thus could not be refuted simply by questioning a single data source, as had been done for past reported discrepancies. This stimulated a dedicated aircraft field campaign called the Atmospheric Radiation Measurement (ARM) Enhanced Shortwave Experiment (ARESE), which seemed to confirm the finding of excess (relative to model predictions) absorption of solar radiation by clouds [*Valero et al.*, 1997a, b; *Zender et al.*, 1997; *Cess et al.*, 1999;

Arking, 1999]. Also, *Wild et al.* [1995] showed that the best current data set (Global Energy Balance Archive (GEBA)) for global annual mean observed solar radiation at the surface disagrees substantially with radiative transfer models used in climate models. Nine climate models produce a range of $164\text{--}185 \text{ Wm}^{-2}$ for this quantity, while the GEBA data set yields 142 Wm^{-2} .

Francis et al. [1997], *Hayasaka et al.* [1995a, b], *Imre et al.* [1996], *Li and Moreau* [1996], *Li et al.* [1997], and *Stephens* [1996] disagree with the findings of excess absorption. Both *Francis et al.* [1997] and *Hayasaka et al.* [1995a, b] presented analyses of field observations showing perhaps some but much less excess absorption than is found in the ARESE studies. *Imre et al.* [1996] and *Stephens* [1996] used methods different from those used by *Cess et al.* [1995] and contend that there is no excess absorption. *Li and Moreau* [1996] and *Li et al.* [1997] used satellite data and a clear-sky radiative transfer algorithm to question the excess absorption. They ascribe any observed, unexplained absorption to aerosols deriving from biomass burning and other sources.

There is also debate over whether there is excess absorption in clear skies. *Arking* [1996] found clear-sky absorption exceeding that predicted by models, while others reached a similar conclusion on the basis of analyses of a large database from the Oklahoma ARM site [*Kato et al.*, 1997, *Halthore et al.*, 1998]. On the other hand, *Zender et al.* [1997] and *Valero and Bush* [1999] detected no excess atmospheric absorption in clear skies beyond the bounds of the model and observational errors. *Charlock et al.* [1998] derived major excess absorption for both

¹Atmospheric Research Laboratory, Center for Atmospheric Sciences, Scripps Institution of Oceanography, University of California, San Diego, La Jolla.

²Atmospheric Sciences Division, NASA Langley Research Center, Hampton, Virginia.

³AS&M, Inc., Hampton, Virginia.

Copyright 2000 by the American Geophysical Union.

Paper number 1999JD901063.
0148-0227/00/1999JD901063\$09.00

clear and cloudy skies from analyses of Oklahoma ARM surface and satellite data. The various results showing anomalously large clear-sky absorption are mainly based on surface insolation measurements. *Bush et al.* [1999a] and R. D. Cess et al. (Consistencies and inconsistencies in measured total, direct, and diffuse shortwave radiation at the surface, submitted to *Journal of Geophysical Research*, 1999, hereinafter referred to as Cess et al., submitted manuscript, 1999) find that it is likely that some surface insolation measurements, in particular the diffuse radiation data, may be affected by significant systematic errors inherent to some of the instruments. *Crisp* [1997] maintains that the traditional radiative transfer models are incorrect and that if correctly done, they would show greater absorption more in agreement with observations.

If the excess absorption by clouds really exists, it should be manifested as anomalous near-infrared to total albedo ratios when compared to traditional models of reflected irradiance unless the excess absorption in the near infrared and in the visible is such that the ratio is unchanged. *Collins* [1998] found that the albedo ratios derived from Nimbus 7 (Earth Radiation Budget (ERB) observations) and the National Center for Atmospheric Research (NCAR) Community Climate Model, Version 3 (CCM3) diverge monotonically as broadband albedo and cloud cover increase. The discrepancy occurs at all latitudes with ice-free oceans during all seasons and is highly statistically significant for each year in the observational record. These results are consistent with enhanced short-wave absorption in cloudy, but not cloud-free, atmospheres. Absorption discrepancies are now seen by many, but major uncertainties remain regarding both the magnitude of the excess absorption and the situations (clear, cloudy, or both) in which it occurs.

The traditional point of view, based on current theory, is that radiation models correctly predict that the atmosphere absorbs, on average, $\sim 20\%$ [*Kiehl et al.*, 1995] of the solar energy arriving at the Earth and that the magnitude of the (broadband, globally annually averaged) absorption is minimally affected by clouds. Some of the recent studies, noted earlier, estimate that the average atmospheric absorption is close to 28% and is greatly affected by clouds. The 8% difference between the two alternative energy budgets is currently the largest uncertainty in the entire climatic energy budget. If the larger figure is true, it has major consequences for our understanding of rainfall, planetary circulation, and indeed the entire Earth system.

From the above discussion one may conclude that there is currently a major question in climate studies. That is, How much solar energy is absorbed in the Earth's atmosphere?

So far, a good deal of the scientific effort has involved studying discrepancies between observations and trying to assign measurement errors to explain the excess absorption. The approach used here, in contrast, is to concentrate on the analysis of ARESE data for those cases that show consistency between totally independent measurements made from the surface, a satellite, and three aircraft.

In summary, this paper presents the results of an analysis of data acquired simultaneously by 15 different instruments from five independent platforms. The following sections present a description of the observational system and of the data from the different platforms as well as a discussion and comparison of the data sets with the purpose of investigating consistency and establishing error estimates. Absorptance is computed for cloudy and clear skies using different methods. The experi-

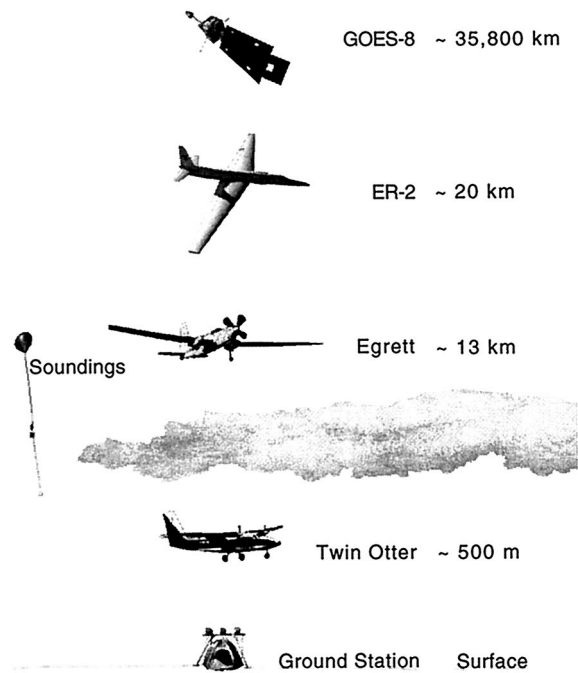


Figure 1. Observational platforms used in Atmospheric Radiation Measurement (ARM) Enhanced Shortwave Experiment (ARESE).

mental values, including retrievals of cloud properties using GOES 8 and surface data, are compared with calculations with the purpose of checking model consistency and model ability to predict the absorption of solar radiation by the atmosphere. The results of previous studies are examined in light of the present findings.

2. Experimental Description

The experimental emphasis of ARESE involved the acquisition of radiometric data by multiple coordinated aircraft and from satellites and surface sites. Three aircraft measured upwelling and downwelling solar radiative fluxes at altitudes ranging from the lower stratosphere to the low troposphere. Flux measurements were also made from the ARM cloud and radiation testbed (CART) central facility located at 97.48° longitude and 36.59° latitude and from secondary surface stations (extended facilities) that are part of the ARM Southern Great Plains (SGP) site. Broadband shortwave top of the atmosphere (TOA) albedos were derived from visible channel radiances from GOES 8.

The ARESE observational system is illustrated schematically in Figure 1. The aircraft, stacked at different altitudes, flew tracks over the surface stations, while the GOES 8 data were taken at a 1 km resolution along the flight tracks every 15 min. In this manner it was possible to obtain coeval measurements of radiative fluxes from which the absorption of radiation by the atmospheric layer between two altitudes (the flux divergence) was determined as the difference between the net fluxes at each level in the atmosphere [*Valero et al.*, 1997a, b]. The net radiative flux is the difference between the downwelling and upwelling fluxes at each altitude. Surface observations provided the radiative flux transmitted through the total column, and the GOES 8 data determined the albedo of the entire column.

The basic instruments required to meet the ARESE objectives, in addition to the CART site facilities and GOES 8, are included in the Radiation Measurement System (RAMS). The RAMS is an array of radiometers covering the spectrum from the near ultraviolet to the far (thermal) infrared. Components of the RAMS vary depending on the purpose and platform being used. The experimental apparatus and methods to acquire airborne and surface data from the RAMS were detailed by Valero *et al.* [1997a, b]. In this study, pairs of the RAMS total solar broadband radiometer (TSBR) and fractional solar broadband radiometer (FSBR) were used for simultaneously viewing in the zenith and nadir directions from each platform. The TSBR and FSBR cover the spectral ranges from 0.224 to 3.91 μm and from 0.68 to 3.3 μm , respectively [Valero *et al.*, 1997b].

Radiative flux measurements in the stratosphere, the upper troposphere, and the lower troposphere were made using the RAMS on the NASA ER 2, a Grob Egrett, and a Twin Otter aircraft, respectively. The Egrett also carried a nadir-viewing scanning spectral polarimeter (SSP) [Partain *et al.*, 1998; Stephens *et al.*, 1999]. Additionally, the RAMS system was installed at three ARM CART surface sites [Bush *et al.*, 1999a].

The RAMS broadband radiometers were calibrated before, during, and after the experiment. The calibration included power calibration, angular response calibration, and spectral response calibration [Valero *et al.*, 1997b]. The calibration accuracy of the broadband radiometers is $\sim 1\%$. The in-flight accuracy is somewhat lower, $\sim 1.5\%$, because of the uncertainties introduced by the pitch and roll movements of the aircraft that affect mostly the direct downward component of the solar flux. A correction is applied to minimize such uncertainties [Hammer *et al.*, 1991; Valero *et al.*, 1997b].

The precision of the airborne measurement was tested in flight during ARESE [Valero *et al.*, 1997b]. The Egrett and Twin Otter were flown at the same altitude and as close to each other as possible for a side by side comparison of the zenith and nadir radiometers. The observed differences between corresponding radiometers in each aircraft were not larger than 5 Wm^{-2} . The average difference for all tested radiometers was $\sim 2\text{--}3 \text{ Wm}^{-2}$. For operational reasons it was impossible to fly the ER 2 side by side with the other aircraft. However, the radiometers were rotated between aircraft and the surface during the experiment, providing at least a partial check on the ER 2 radiometers.

An additional check of instrument accuracy was done during ARESE by periodic comparisons with an absolute cavity radiometer, the same one used for the power calibrations and traceable to the World Radiation Reference Standard. Further RAMS broadband accuracy checks were made during the Subsonic Aircraft Contrail and Cloud Effects Special Study (SUCCESS) [Valero and Bush, 1999] by Wiscombe *et al.* [1998] and Bush and Valero [1999].

3. RAMS Data

The aircraft flight tracks over the CART site during the 4 days selected for this study are shown in Figure 2. Figures 3–6 are time series of 1 s mean net fluxes from the Egrett and Twin Otter that were used to determine the absorptance for clear-sky and cloudy conditions. Figure 3 (October 11) depicts clear-sky conditions, while Figures 4–6 (September 25, October 13, and November 1, respectively) display varying degrees of cloud

cover. During September 25, October 13, and November 1, there were periods of clear sky, broken clouds, and overcast skies. The GOES 8 image in Figure 7 shows the cloud cover on November 1, for example. The combinations of cloud conditions observed during the same flight are very useful for comparing the relative effects of varying cloud cover on the radiation field while minimizing the potential instrumental changes between observations. On such flights the differences between cloudy and clear conditions, which constitute the fundamental point of this research, become relative measurements dependent mostly on precision, rather than absolute measurements, demanding precision plus accuracy.

The data gaps in Figures 3–6 correspond to times when the Twin Otter was refueling or when the Egrett was turning to maintain coordination with the Twin Otter. At the Egrett's altitude of 13 km its ground speed is greater than that of the Twin Otter, so the Egrett made periodic 360° turns in order to maintain a horizontal separation between the two aircraft of 1 km or less. These maneuvers were described by Valero *et al.* [1997a, b]. These 360° turns can be seen as loops in Figure 2. All data points outside the 1 km range were eliminated from the analysis to assure collocation. The cumulative averaging of the data (section 6.2) takes care of small collocation offsets within the 1 km requirement [Marshak *et al.*, 1997].

The fluxes measured from aircraft are used to estimate atmospheric absorptance for comparison to model calculations. S. K. Pope and F. P. J. Valero (Observations and models of flux profiles, column transmittance, and column reflectance during ARESE, submitted to *Journal of Geophysical Research*, 1999, hereinafter referred to as Pope and Valero, submitted manuscript, 1999) compared calculated and measured downwelling fluxes at 13 km in order to examine the observed day-to-day and shorter timescale variability in the downwelling fluxes measured from the Egrett. For both day-to-day and instantaneous variability they found agreement between modeled and measured downwelling fluxes. They confirmed that such variations are largely a consequence of multiple scattering, which in turn depends on the optical depth and optical depth variability above and below the aircraft flight level. The creation of substantial diffuse upwelling radiation by a high-albedo surface causes additional downwelling radiation by the backscattering action of the gases and any aerosols in the atmosphere above the aircraft. Pope and Valero (submitted manuscript, 1999) showed that even at 13 km, the multiple-scattering effects of the atmosphere above the aircraft on the downwelling fluxes are significant and can reach values of $10\text{--}20 \text{ Wm}^{-2}$ and possibly higher. The magnitude of the enhancement and variability in the downwelling fluxes depends on the atmospheric conditions not only above but also below the aircraft (clouds, aerosol loading, surface and cloud albedo, etc.). The Pope and Valero (submitted manuscript, 1999) analysis, together with the "wing to wing" comparisons described by Valero *et al.* [1997b] and the following GOES 8 comparisons, constitutes a check for the sensitivity, dynamic range, precision, and accuracy of the RAMS aircraft instruments, which provide much of the data used in the following analyses.

For surface radiative fluxes we use the RAMS TSBR, specially installed at the CART central facility during ARESE, rather than the CART site radiometers that were also operated during ARESE. This decision was based on studies by Morikofer [1939], Bener [1950], Drummond and Roche [1965], Robinson [1966], Rodskjer [1971], Gulbrandsen

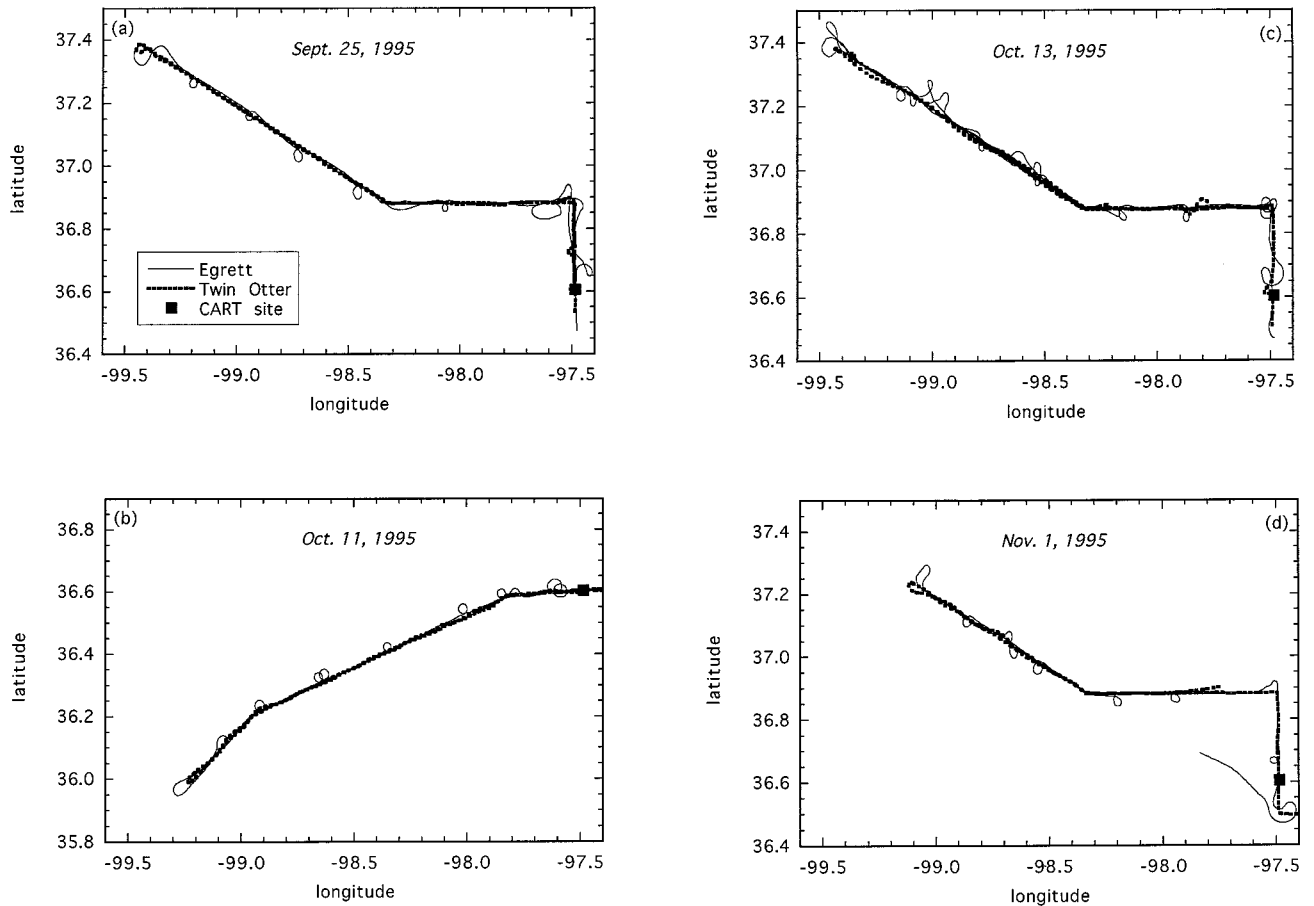


Figure 2. Aircraft latitude is plotted versus longitude to illustrate the flight paths for the 4 days analyzed in this study: (a) September 25, 1995, (b) October 11, 1995, (c) October 13, 1995, and (d) November 1, 1995. The Southern Great Plains cloud and radiation testbed (CART) site is indicated by a solid square.

[1978], and more recently, *Bush et al.* [1999b] and Cess et al. (submitted manuscript, 1999). These studies indicate the potential for significant thermally generated errors that affect measurements acquired with radiometers of design similar to those used at the CART site. For such reasons, data from these instruments were used only for comparison purposes.

4. GOES 8 Data

To match the aircraft observations, GOES 8 visible radiances from 1 km pixels were averaged along a 10 min leg of the aircraft flight path. The flight leg was centered on the GOES 8 observing time. The mean GOES 8 visible radiances were then converted to broadband albedos following the procedures out-

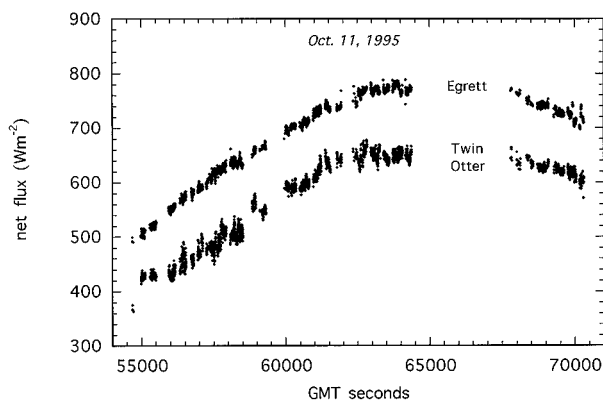


Figure 3. A time series of net fluxes from the EgreTT and Twin Otter that were used to determine the absorptance for October 11, 1995. The data shown are 1 s means.

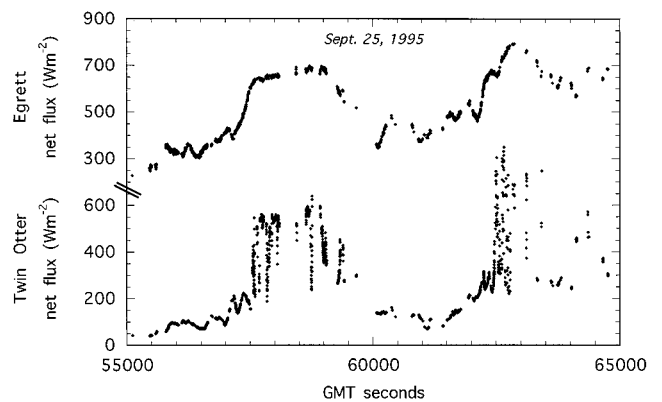


Figure 4. A time series of net fluxes from the EgreTT and Twin Otter that were used to determine the absorptance for September 25, 1995. The data shown are 1 s means.

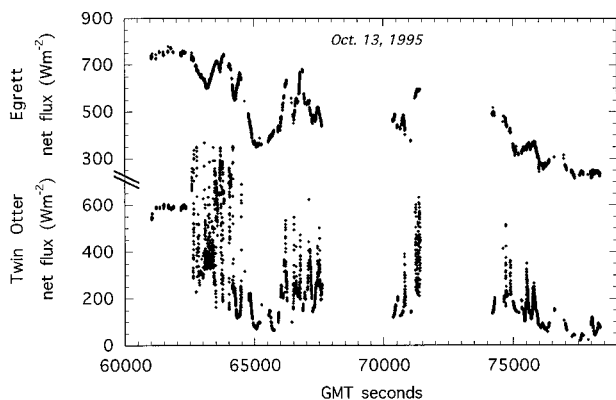


Figure 5. A time series of net fluxes from the Egrett and Twin Otter that were used to determine the absorptance for October 13, 1995. The data shown are 1 s means.

lined by *Minnis et al.* [1995a] and updated by *Minnis and Smith* [1998]. This process uses a regression function between October 1986 GOES 6 visible albedos and the Earth Radiation Budget Experiment (ERBE) Earth Radiation Budget Satellite (ERBS) broadband shortwave (0.2–5.0 μm) scanner (35 km resolution) albedos. Thus the GOES-derived albedos should be representative of the values expected from ERBE. *Minnis et al.* [1995a] and *Minnis and Smith* [1998] discuss in detail the use of a single regression function for both clear and cloudy skies. The procedures followed include the use of separate bidirectional correction factors for clear and cloudy pixels and also include the determination of cloud fraction from the satellite data.

Preliminary estimates of the uncertainties in the broadband shortwave albedos derived with GOES visible channel data taken over the ARM SGP domain have been determined using several approaches [*Doelling et al.*, 1998, 1999] including initial comparisons with Egrett, Twin Otter, and ER 2 RAMS data taken during ARESE. Three independent satellite data sets, including the 1000 km resolution ERBS wide field of view (WFOV) and the Clouds and Earth Radiant Energy System (CERES) albedos [*Wielicki et al.*, 1998], were also matched to coincident GOES 7 and GOES 8 broadband albedos at various times between 1994 and 1998. During the ARESE period, only 5 ERBE data points could be matched with GOES 8 during the

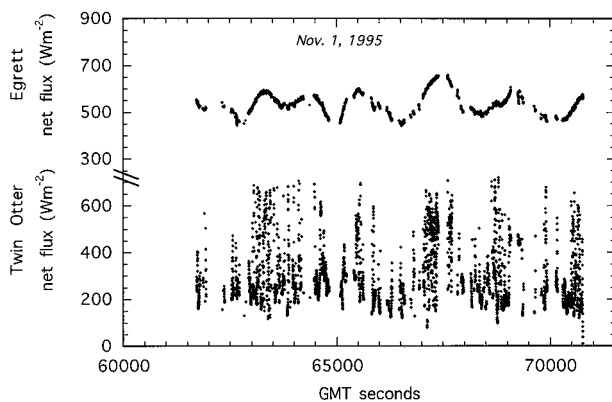


Figure 6. A time series of net fluxes from the Egrett and Twin Otter that were used to determine the absorptance for November 1, 1995. The data shown are 1 s means.

day. The instantaneous GOES 8 albedos were 0.022 ± 0.053 greater than those derived from ERBS WFOV data during ARESE [*Doelling et al.*, 1998]. The mean difference is not statistically different from zero. A more reliable comparison uses all of the ERBE data through 1998. The mean difference between the ERBE WFOV and GOES 8 between 1994 and 1998 is -0.012 ± 0.033 [*Doelling et al.*, 1999]. Much of the uncertainty in the GOES WFOV differences results from errors in matching the data sets and the small sample numbers. The mean difference between GOES 8 and the CERES on the Tropical Rainfall Measuring Mission satellite (TRMM) is -0.001 ± 0.030 for the period between January and August 1998.

While few of the satellite comparisons were performed for the ARESE period, they represent the typical performance for the GOES 8 broadband albedos. Furthermore, the uncertainties are generally very close to those expected from the process of converting radiance to flux with anisotropic correction factors. Thus no systematic errors are expected to occur in the GOES 8 albedos unless the visible channel calibration varies in an unpredictable fashion. *Ayers et al.* [1998] and *Nguyen et al.* [1999] used the NOAA 14 advanced very high resolution radiometer (AVHRR) as a reference for calibrating the GOES 8 visible channel. This calibration source has been tracked continuously since the launch of the NOAA 14, and its calibration coefficients have been updated to account for degradation of the sensor. The accuracy of this calibration was confirmed independently several times using a variety of sources including the Antarctic snow surface [*Loeb*, 1997] as well as the Advanced Tropospheric Scanning Radiometer (N. Rao, personal communication, 1998) and the Visible Infrared Scanner on TRMM [*Nguyen et al.*, 1999]. These latter instruments use onboard calibration systems that permit views of the Sun through well-characterized diffuser plates. Thus the degradation of the NOAA 14 visible channel sensitivity is well established. By performing calibrations against NOAA 14 every few months, *Ayers et al.* [1998] showed that the GOES 8 visible channel has degraded in a predictable linear fashion since it began operations in 1995. The GOES 8 gain (0.656) used here is based on an update of that calibration degradation curve using the latest NOAA 14 AVHRR calibration. The AVHRR GOES 8 calibration closest to the ARESE period that contributed to the degradation curve was performed during August 1995. The slope of the degradation curve is precise to within $\pm 5\%$ between 1995 and 1998.

To establish that there were no short-term variations in the GOES-8 gain, the clear-sky visible channel albedo was derived over the CART site every day during ARESE when possible. The results plotted in Figure 8 show that except for October 3 the albedo varied by <0.003 for a given solar zenith angle during the morning and by <0.01 during the afternoon for solar zenith angles $<60^\circ$ (the albedos used here). A heavy rainfall occurred during October 2 that substantially increased the surface moisture. Soil moisture levels rapidly returned to a nearly constant level for the remainder of the month [*Lin and Minnis*, 1999]. The separation in the albedo is due to two sources, morning dew and errors in the models used to correct the radiances for anisotropic reflectance [*Minnis et al.*, 1997]. The consistency of the morning albedos and the variability of their afternoon counterparts suggest that surface soil moisture and dew are the primary source of the diurnal differences. For example, during October 3, when the surface moisture is relatively high all day, the differences between the morning and

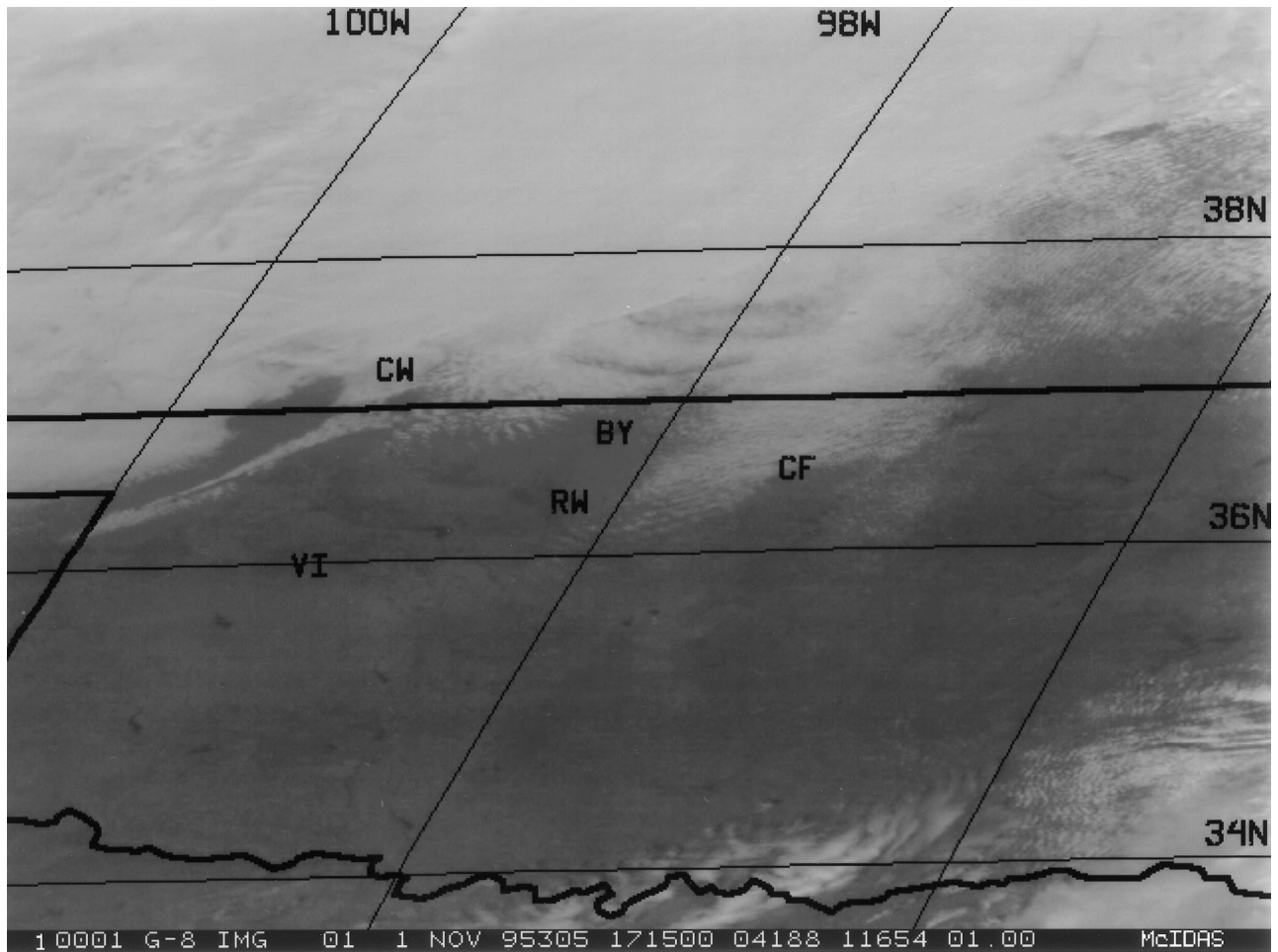


Figure 7. GOES 8 visible image for November 1, 1995, at 1715 UTC. The image has 1 km resolution and is centered over the CART site (indicated by CF). The ARM extended facilities of Byron (BY), Ringwood (RW), Vici (VI), and Coldwater (CW) are also shown.

afternoon albedos are <0.01 . This interpretation is consistent with observations of microwave surface emissivity during ARESE that show a significant diurnal cycle that corresponds to a wet surface during the morning and a dry surface during the afternoon [Lin and Minnis, 1999]. This diurnal cycle was absent during October 3. Given these physical variations and the consistency of the morning albedos observed with GOES 8, it is concluded that the GOES 8 visible channel calibration is stable throughout the ARESE period.

5. Radiative Transfer Model

The discrete ordinates radiative transfer algorithm [Stamnes *et al.*, 1988] is used to calculate the theoretical (“modeled”) absorptance corresponding to the observations. The solar spectrum is divided into 185 bands, and gaseous absorption is computed using exponential sum fits [Lubin and Simpson, 1997]. Of the 185 spectral bands in the model, 41 are in the visible (i.e., are short of $0.7 \mu\text{m}$). The model solar zenith angle was set to 54° , which was the average during the ARESE time period. Sondes launched from the SGP CART site during ARESE were used to get pressure, temperature, ozone, and relative humidity profiles appropriate for the day and time of each flight. Cloud and aerosol properties were implemented in

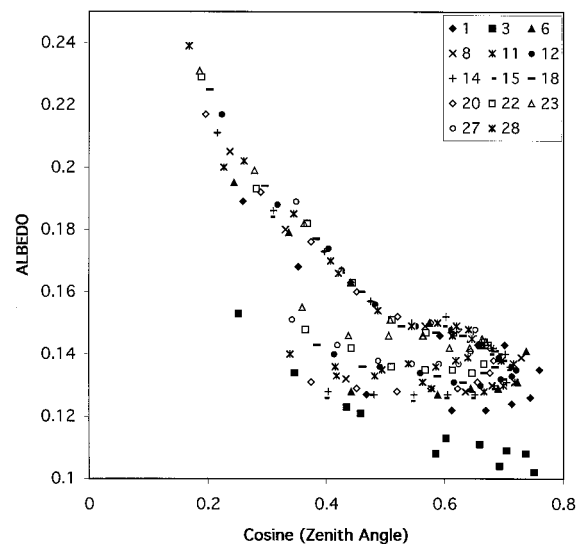


Figure 8. GOES 8 visible clear-sky albedos are plotted versus cosine of solar zenith angle to illustrate the stability of the albedo retrievals. Each day in October 1995 is plotted with a different symbol; the data points for October 3 correspond to a moist surface after precipitation.

the model by specifying single-scattering albedo, asymmetry factor, and volume extinction coefficient as functions of wavelength. The cloud particles were assumed to be $10\ \mu\text{m}$ water droplets. A range of optical depths consistent with values observed during ARESE was assumed for cloudy conditions. A range of aerosol types was used, including rural aerosol, mineral dust aerosol, and soot aerosol (likely at the CART site because of biomass burning activities (Valero and Bush, submitted manuscript, 1999). Pope and Valero (submitted manuscript, 1999) give further details of the model calculations. The model calculations yield overcast absorptance values ranging from 0.16 to 0.24, depending on the cloud and aerosol implementation. The narrow band model calculations by Zender *et al.* [1997] were also used for comparison purposes.

6. Data Analysis

6.1. Comparisons of GOES 8 and Aircraft Albedos

To compare aircraft and satellite albedos, it is necessary to adjust the satellite albedos to flight level or the aircraft data to the TOA. Here the latter process was implemented using correction ratios based on radiative transfer computations using the method of Fu and Liou [1993]. The model uses profiles of atmospheric properties for the period archived as by Charlock and Alberta [1996] to compute the TOA albedo given the albedo measured at an altitude. The profiles include soundings taken over the experimental site every three hours and the aerosol optical depths also measured at the site. Correction factors are the ratios of the computed TOA albedos to those at a particular level such as flight altitudes [Doelling *et al.*, 1997]. These ratios are then applied to the mean TSBR albedos along the 10 min flight leg. The mean TSBR albedos were computed by separately summing the downwelling and upwelling fluxes for the leg and computing the ratio of the upwelling to downwelling sums.

The TOA albedo correction is not very sensitive to humidity errors. For the Twin Otter the TOA albedo varies by no more than 0.007 out of 0.3 for a 25% error in the column water vapor. That error is the extreme value for a low Sun and high surface albedo. For the Egrett and the ER 2 the relative error for a 25% humidity error is $<0.1\%$. Thus humidity errors have minimal impact.

Figure 9 shows a comparison of albedos measured simultaneously from GOES 8 and the three aircraft flying over the CART site during various days of ARESE. The ER 2 comparison (Figure 9a) includes data from days prior to October 23 because the ER 2 did not fly after that date. The ER 2 and Twin Otter (Figure 9b) comparisons with GOES 8 show good agreement in every case considered (well within the experimental errors). The comparisons between the Twin Otter and GOES 8 are limited to clear days because the Twin Otter always flew below clouds when they occurred. The ER 2 comparisons apply to a variety of clear and cloudy conditions and are particularly useful and reliable because the atmospheric corrections are minimal because of the high altitude of the ER 2. Instantaneously, the GOES 8 albedos are 0.013 ± 0.016 greater than the ER 2 results and 0.006 ± 0.011 less than the Twin Otter albedos. The GOES 8 albedos also agree well with the Egrett-measured albedos (Figure 9c) during 4 days: September 25, October 11, October 13, and November 1, which represent 40% of the total coordinated flight time during ARESE. However, there appears to be poorer agreement between

the Egrett TSBR and GOES 8 for other days as seen by Doelling *et al.* [1999]. The GOES 8 albedos are 0.018 ± 0.032 greater than the Egrett albedos on an instantaneous basis.

The above comparisons indicated good stability of the GOES 8 measurements with respect to observations from the Twin Otter and ER 2 TSBRs and also to the Egrett TSBR during the 4 selected days noted above. Given the stability of the GOES 8 observations and their consistent comparisons with the ER 2, Twin Otter, and Egrett, it is concluded that the fluxes for September 25, October 11 and 13, and November 1 form a consistent data set.

6.2. Absorption of Solar Radiation by the Atmosphere

The data were analyzed following both the radiative flux divergence approach and the reflectance R versus transmittance T "slope" method [Cess *et al.*, 1995; Pilewskie and Valero 1995, 1996]. The mean absorption in the column was computed for each day by first calculating the net flux at each aircraft level using 10 s averages of each measurement. Then the net flux at the Twin Otter altitude was subtracted from the Egrett net flux to yield the absorption. Before using the mean values it was necessary to minimize the sampling errors related to the variability and three-dimensional effects of clouds on the radiative fluxes. We applied the methods discussed by Marshak *et al.* [1997] to compute flight time-averaged absorptance. Each data set was tested to ensure that temporal averaging was sufficient to eliminate sampling errors associated with broken clouds and other three-dimensional cloud reflectance effects. The results in Figure 10 show cumulative averages of the absorptance between the two aircraft (column cumulative average absorptance divided by the TOA cumulative average insolation) for each day versus averaging time. The standard deviations of the average are noted in Figure 10; they do not include uncertainties in calibration and navigational errors. To confirm that the mean absorptance converges within the experimental and sampling errors to a unique asymptotic value, the cumulative averages were computed in four different ways by rotating the order of the data points, as done by Valero *et al.* [1997a]. First, the averaging was performed following the time sequence of the data. Second, the first 25% of the data were moved to the end of the data sequence. Third, the first 50% of the data were moved to the end, and finally, the first 75% of the data were moved. Figure 11 depicts examples of the results of this analysis for September 25 and November 1 and demonstrates the uniqueness of the mean absorptance, consistent with the standard deviation. This implies that the sampling errors have been averaged out to an acceptable level and further indicates that the sample is large enough to represent realistically the mean absorptance.

Figure 12 shows the whole flight averages of the total solar and near-infrared absorptance (Figure 12a) and transmittance (Figure 12b) measured for the 4 selected days. Some near-infrared values are missing because the Egrett FSBRs were not operational on September 25, and the Egrett nadir FSBR failed on October 11.

The data set was also analyzed by classifying it in three subsets according to sky condition: clear, broken clouds, and overcast. The data from the 4 days were put into one of three bins by looking at the time series of fluxes. Since the two aircraft flew in coordination, the fluxes from both the upper and the lower aircraft change when the cloud amount in the column in between them changes. This provides a distinctive signature for the three bins relative to one another. When

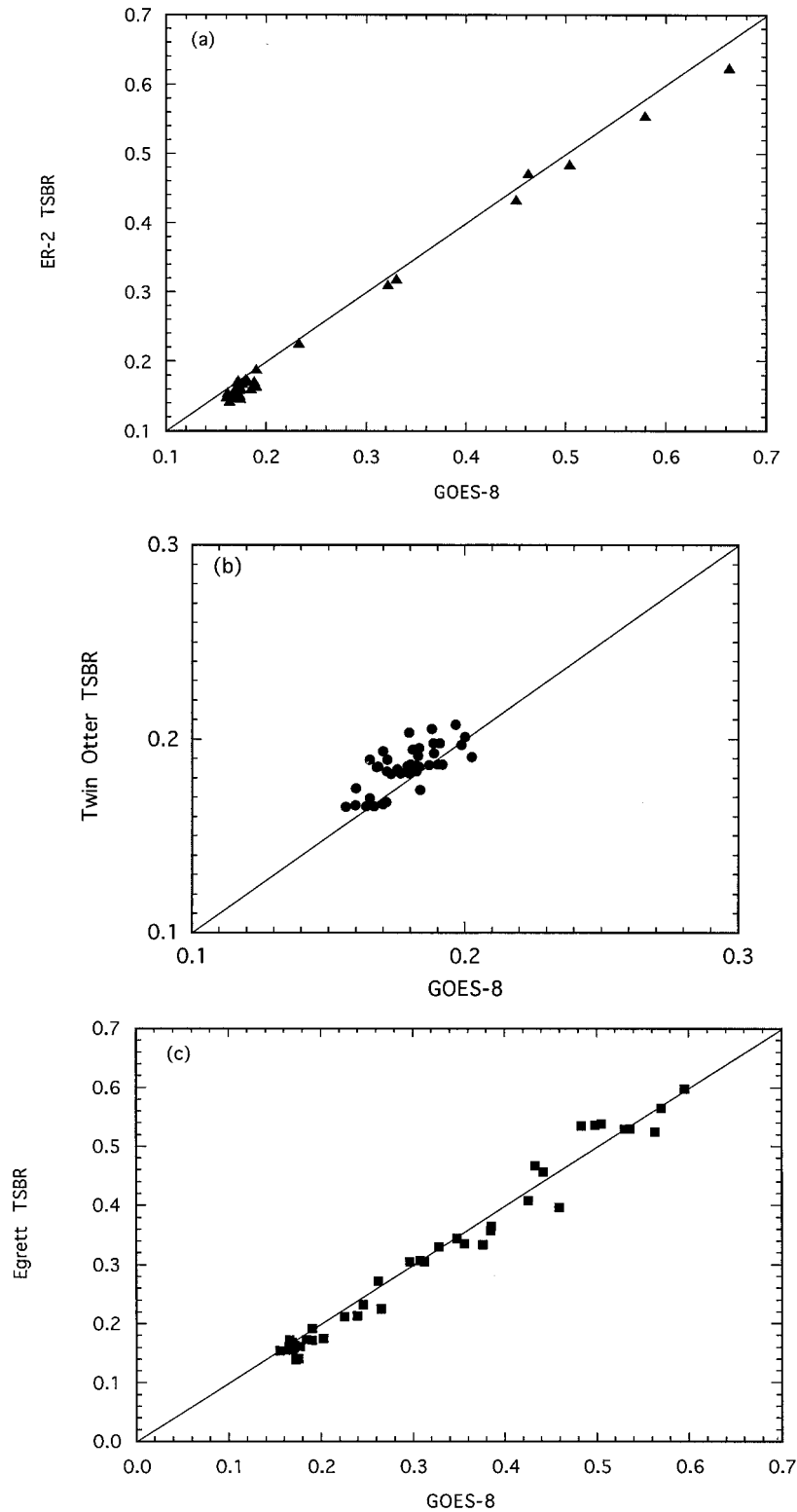


Figure 9. Comparison of albedos measured simultaneously (10 min averages) from GOES 8 and from (a) ER 2, (b) Twin Otter, and (c) Egrett. Figures 9a and 9b include all data available during ARESE, while Figure 9c is limited to September 25, October 11, October 13, and November 1, 1995. See explanation in text.

there is a thick cloud the fluxes vary little with time, the upper aircraft upwelling flux is high, and the lower aircraft downwelling flux is low. These data were put into the “overcast” bin. When there is no cloud, the fluxes also vary little with time, but

the upper aircraft upwelling flux is low, and the lower aircraft downwelling flux is high. These data were put into the “clear-sky” bin. In conditions of scattered to broken clouds the fluxes seen by the two aircraft vary more rapidly; these data were put

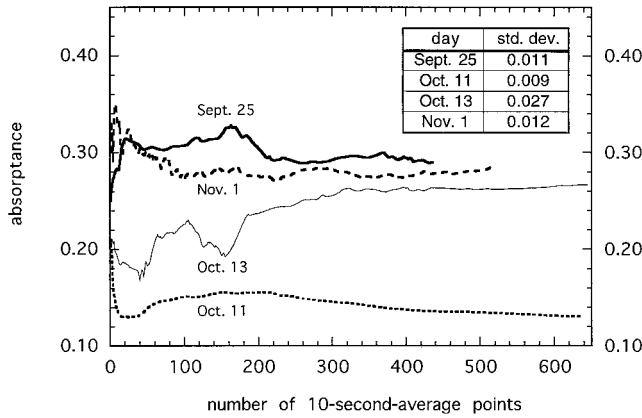


Figure 10. The Egrett-Twin Otter column absorptance evaluated from collocated 10 s mean TSBP measurements as a function of a cumulative number of points for September 25, October 11, October 13, and November 1, 1995. The endpoint of each curve is the mean absorptance for that day. The standard deviations are shown in the table.

into the “broken clouds” bin. In this way the data from the four flights were put into bins, in sections no shorter than 40 s and typically much longer in duration. With the data binned in this way the same sampling analysis described above was performed. Again, it was found that the sampling was sufficient for convergence to a stable value of absorptance. Figure 13 depicts cumulative averages and standard deviations that correspond to this analysis, and Figure 14 shows the absorptance and transmittance values that result. Absorptance increases with increasing cloud cover, as found in previous work. A model

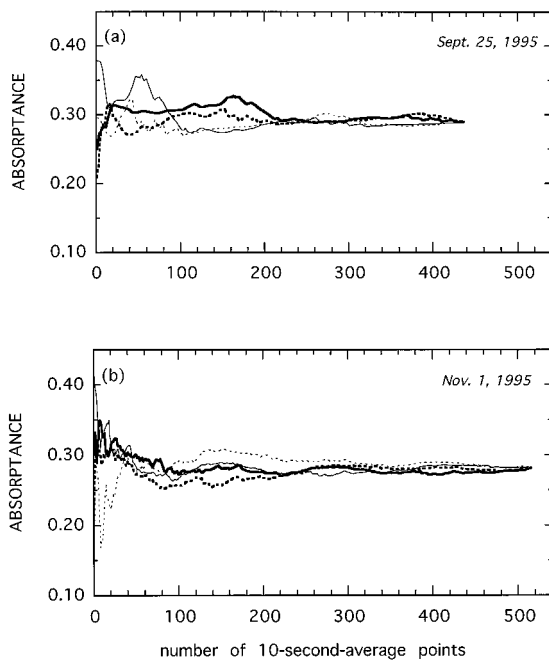


Figure 11. Cumulative absorptance for the Egrett-Twin Otter column computed in four different ways by rotating the order of the data points as explained in the text for (a) September 25 and (b) November 1. Convergence to a common value indicates that the sampling is enough to achieve a stable value for the absorptance.

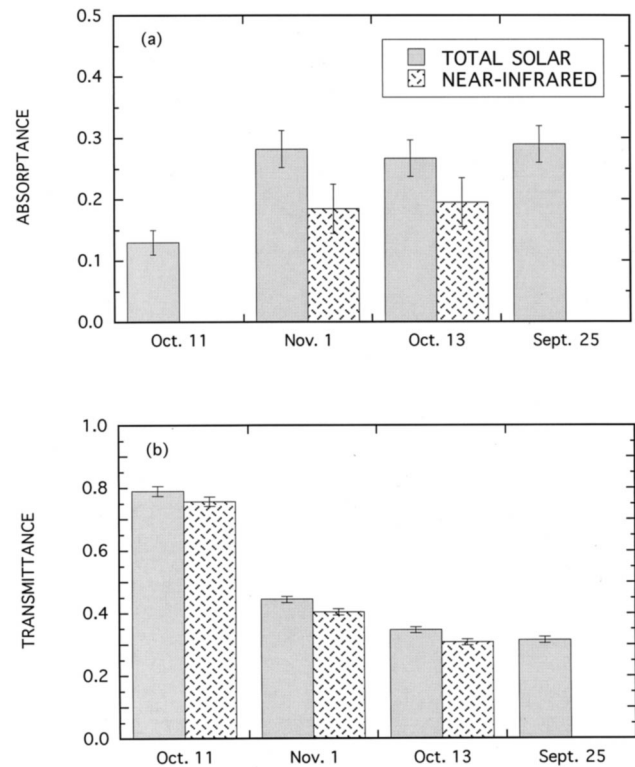


Figure 12. Whole-flight averages of the total solar and near-infrared (a) absorptance and (b) transmittance for the 4 days discussed in this paper.

and measurement comparison is shown in Figure 15 confirming the difference between calculated and measured absorptance of solar radiation by the cloudy atmosphere. While the data show a marked increase of absorptance with cloud cover, the model is less sensitive to clouds, as found in previous studies.

It should be emphasized here that these results point to a visible excess absorptance smaller than that reported previously [Zender *et al.*, 1997; Valero *et al.*, 1997a]. Now it is found that for overcast conditions the absorptance in the 0.224–0.68 μm spectral region (estimated as the difference between the

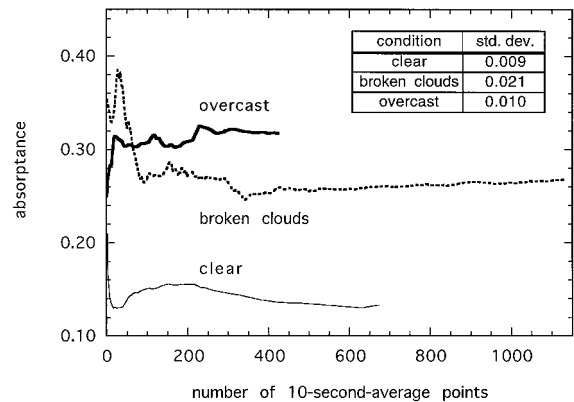


Figure 13. The Egrett-Twin Otter column absorptance evaluated as in Figure 11 but for the data classified according to clear, broken clouds, and overcast conditions. The table shows the corresponding standard deviations.

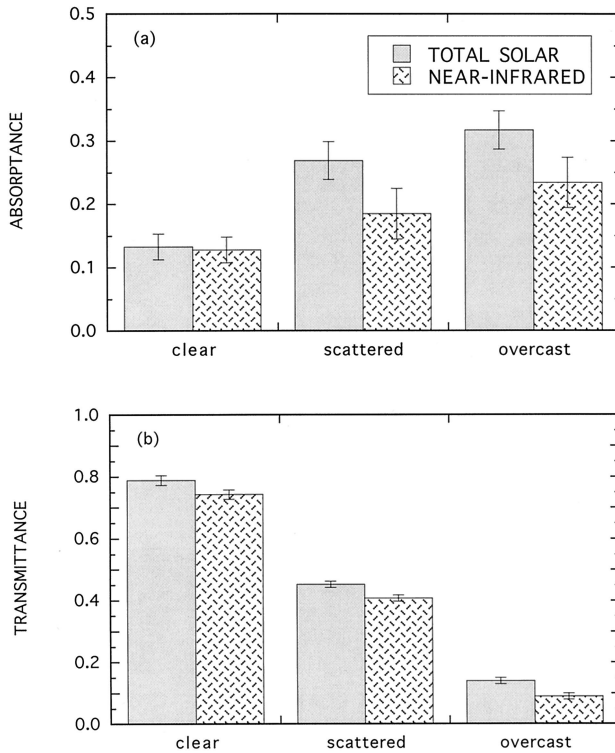


Figure 14. Absorptance and transmittance computed by binning the data from the 4 days into three bins corresponding to clear, broken clouds (scattered), and overcast conditions.

total and the near-infrared absorptances) is $\sim 0.08 \pm 0.06$. Furthermore, not all of this ultraviolet visible absorptance can be attributed exclusively to clouds since significant aerosol effects may be present, as suggested by the 500 nm absorptance of ~ 0.05 reported by Valero *et al.* [1997a].

6.3. Top of the Atmosphere Albedo (GOES 8) versus Surface Transmittance (RAMS)

Another way to view the data is to compare the slopes of the lines on the basis of a regression of TOA albedo versus transmittance at the surface for observations and model calculations [Cess *et al.*, 1995]. An additional feature of this comparison is that it incorporates still another platform, the surface, to the overall analysis presented in this paper. The results are shown in Figure 16 for matched GOES 8 albedos for a 0.3° box centered over the CART site and transmittances from the uplooking RAMS TSBR at the surface for the entire ARESE period. The model gives a slope of ~ -0.8 , while a linear fit to the observations yields a mean slope of -0.61 ± 0.02 with a linear correlation coefficient of 0.97. From the plot an atmospheric (surface to TOA) absorptance of ~ 0.33 is obtained for a surface albedo of 0.19 (determined from Twin Otter observations during ARESE) and a transmittance of 0.20 (overcast conditions). The absorptance is estimated with the relationship (see Appendix 1):

$$R_{\text{layer+surface}} + T_{\text{layer}} + A_{\text{layer}} = 1 + \alpha T_{\text{layer}}, \quad (1)$$

where $R_{\text{layer+surface}}$, T_{layer} , A_{layer} , and α stand for reflectance of the surface plus the layer, layer transmittance, layer absorptance, and surface albedo, respectively.

The surface RAMS TSBR data were only available for 12

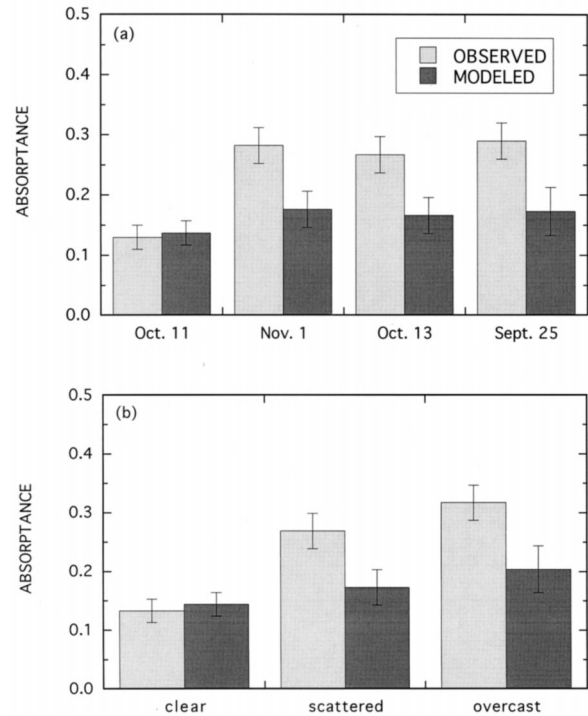


Figure 15. Comparison of model-calculated and measured absorptance for the Egrett-Twin Otter column is shown for (a) the 4 days October 11, September 25, October 13, and November 1, 1995. The measured values are whole-flight averages with error bars shown. The model value for each day is the average of models run for that day with varying cloud amount. The error bars on these values represent the range of absorptances that result from all the models run. (b) the same 4 days' data are binned by sky condition. While the data show a marked increase of absorptance with the cloud cover, the model is less sensitive to clouds as predicted by theory.

days after October 10. The ARM (SIROS) radiometer operated continuously throughout the experiment while ARM BSRN radiometer collected data for various days during ARESE. For comparison purposes, the slopes were also computed using the Solar and IR Observation Stations (SIROS) and Baseline Surface Radiation Network (BSRN) data sets. The average slopes are -0.64 ± 0.03 and -0.64 ± 0.10 for the SIROS and BSRN, respectively. The BSRN data set contained few cloudy points, resulting in the larger uncertainty.

7. Discussion and Comparison With Other Results From ARESE

7.1. October 30

October 30, a heavily overcast day, was previously analyzed by Valero *et al.* [1997a] and by Li *et al.* [1998]. Some large discrepancies between albedos measured by different instruments were noted for this day by Li *et al.* [1998]. The SSP and TSBR albedos differ by 0.144, while the SSP and TSBR albedos differ from GOES 8 by +0.084 and -0.06 , respectively. A comparison of the TSBR absorptance for overcast conditions found in this study (for September 25, October 11, October 13, and November 1) with those reported previously by Valero *et al.* [1997a] for October 30 indicates that the absorptance for October 30 is larger than but still consistent with the present

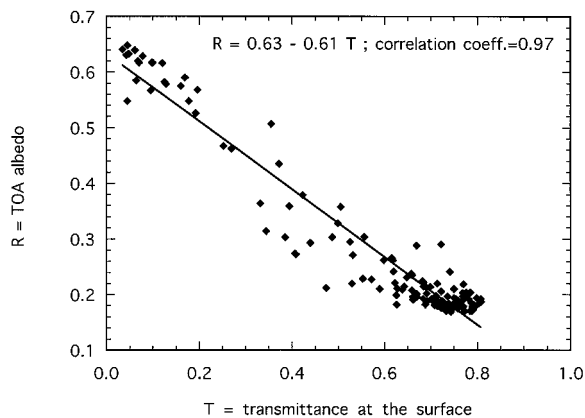


Figure 16. A plot of GOES 8 top of the atmosphere (TOA) albedo versus transmittance at the surface in 10 min averages for the 12 days in which surface data were collected by the RAMS.

results. The October 30 absorptance in the layer between the Egrett and the Twin Otter was 0.36 ± 0.03 , while the present results yield an overcast absorptance of 0.32 ± 0.03 . Given the experimental errors and possible differences in the overcast conditions, such a discrepancy is not surprising.

However, on October 30 the 4 hour mean difference in albedo between GOES 8 and the Egrett TSBR is more than double the standard deviation for the instantaneous differences between the ER 2 and Twin Otter on all other days and between the GOES 8 and the Egrett for the 4 days examined above in this study. Given the stability of the GOES 8 calibration, this large difference suggests that an anomaly in the Egrett aircraft (e.g., localized icing or landing gear oil leaks, which were occasionally noted during the experiment and considered repaired) may have affected both the SSP and TSBR instruments during this flight. Both instruments show exceptionally large differences when compared to the GOES 8 albedos and to each other; the differences are the largest observed during ARESE. On the other hand, the low-altitude wing to wing comparisons of the Egrett and Twin Otter TSBR and FSRB radiometers [Valero *et al.*, 1997b] point to good precision of the instruments. It may be that the wing to wing comparisons, which were limited to altitudes reachable by the Twin Otter, cannot account for changes that may occur at higher altitudes where temperature and pressure are lower.

It has been shown that the GOES 8 albedos are quite stable and accurate during ARESE and that the Egrett albedos appear to be biased low during the October 30 flight. If the October 30 Egrett albedos are corrected to match the GOES 8 albedos, the absorptance in the Egrett-Twin Otter column computed by Valero *et al.* [1997a] reduces from 0.36 ± 0.03 to 0.31 ± 0.04 . While this value is smaller than before, it is still $\sim 30\%$ greater than expected from either the model calculations of Zender *et al.* [1997] or the maximum absorptances calculated in section 6.2 using the discrete ordinates radiative transfer (DISORT) method. Furthermore, the albedo-transmittance slope computed from the October 30 GOES 8 and surface measurements is -0.61 , consistent with the results from the analyses in this study. Thus the conclusion of anomalously high absorption drawn from Zender *et al.* [1997] and Valero *et al.* [1997a] is essentially the same, except for the magnitude and possibly the spectral distribution of the excess

absorption. The near-infrared data from the Egrett were consistent throughout ARESE; the near-infrared absorptance measured on October 30 is $\sim 0.27 \pm 0.04$, which compares well with the near-infrared absorptance of 0.24 ± 0.05 reported in this study. The larger uncertainty in the latter figure results from the smaller number of data points available.

If for October 30 the corrected total absorptance (0.31 ± 0.04) and near-infrared absorptance (0.27 ± 0.04) are used to compute the absorptance in the ultraviolet visible, one obtains the value 0.04 ± 0.06 . This is statistically similar to the 0.08 ± 0.06 value obtained for the 4 days selected for this study and is also consistent with the 500 nm measured absorptance of Valero *et al.* [1997a].

7.2. Differences Between Cloud Properties and Albedos Derived from GOES 8 and the Surface

Differences between the cloud properties and albedos derived from GOES 8 and the surface during the October 30 flights provide another indication of the discrepancy between the model-calculated and observed atmospheric absorption. The cloud liquid water path (LWP) was derived from the uplooking microwave radiometer at the ARM central facility, while the cloud optical depth τ and effective droplet radius r_e were derived simultaneously using the BSRN radiometer and the Pennsylvania State University cloud radar using the method of Dong *et al.* [1997]. These same parameters were derived from the 4 km GOES 8 $0.65 \mu\text{m}$, $3.9 \mu\text{m}$, and $10.8 \mu\text{m}$ data using a strip of 25–40 pixels centered over the central facility extending along the 190° wind vector at 750 mbar. The satellite data were analyzed with the visible-infrared-solar-infrared technique (VIST) described by Minnis *et al.* [1995b] using the parameterizations of Minnis *et al.* [1998]. For the sake of comparing the surface- and satellite-derived cloud properties a two-stream radiative transfer model was used to compute the broadband shortwave albedo at the top of the atmosphere. The results in Figure 17 show that the mean VIST r_e is $4 \mu\text{m}$ greater than the value derived from the surface data. Conversely, the mean surface-based optical depth is 32 compared to 20 from GOES 8. The values agree at 1700 and 1900 UTC. Despite the general disagreement between the corresponding values of τ and r_e , the LWPs are very close with means of 169 and 166 gm^{-2} from GOES 8 and the surface, respectively. The computed albedos from the surface data yield mean values of 0.64 compared to 0.55 derived from the GOES 8 data. The two-stream computations using the VIST results yield a mean broadband albedo of 0.56, which is in excellent agreement with the albedo derived empirically from the visible channel alone.

If the GOES 8 retrievals underestimated τ because of any calibration errors, they would also underestimate LWP because the information in the $3.9 \mu\text{m}$ radiance is independent of τ when τ exceeds 10. Thus the match in LWPs from the surface and satellite in Figure 17 would be extremely fortuitous if τ is underestimated because of a calibration error. The $3.9 \mu\text{m}$ channel calibration would need to be in error just enough to yield a droplet size that produces the correct LWP. Although the shortwave albedo from GOES 8 is not totally independent of the cloud properties derived from the GOES 8 visible and solar infrared channels, it still provides some independent confirmation of the retrievals. The narrowband to broadband conversion uses empirical results with bidirectional correction factors that differ from the plane parallel model used to retrieve τ and compute the albedo from τ . The consistency in LWP and

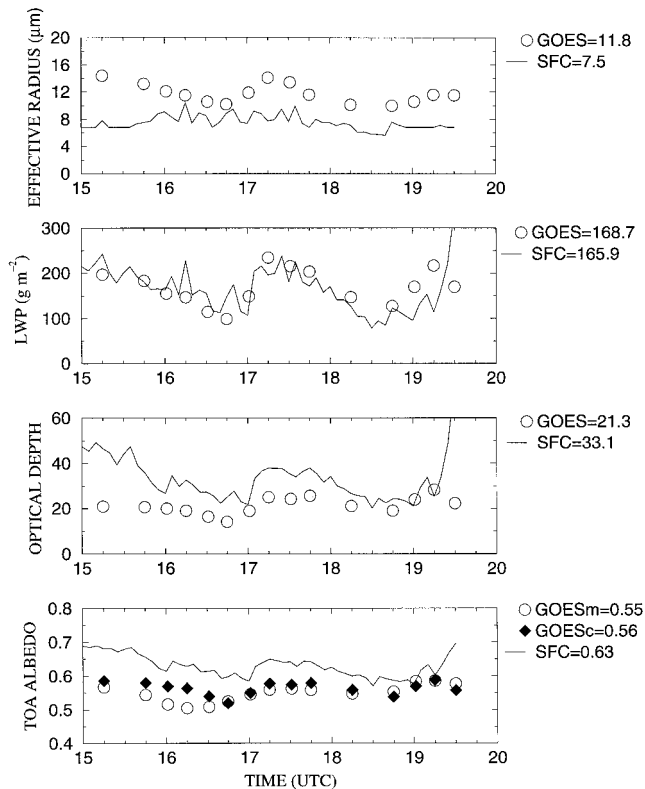


Figure 17. Cloud properties and TOA albedos derived from surface-based measurements and from GOES 8 over the ARM Central Facility during October 30, 1995. GOESm refers to albedo measured from GOES. GOESc refers to albedo computed from GOES-derived cloud properties.

the albedo calculations for GOES 8 lend further credence to the previously discussed assessment of the GOES 8 shortwave albedos.

The larger albedos calculated with the optical depths derived from the surface data are consistent with excess absorption because the models attribute diminished transmittance primarily to increased albedo. Thus excess absorption by clouds would be interpreted as larger optical depths and smaller droplets from analysis of surface radiometer data. Conversely, in the case of excess absorption by the cloud the reflected radiances would yield larger droplets and smaller optical depths when analyzed with the standard radiative transfer models. While it is difficult to determine which values of τ and r_e are correct in this instance, the larger droplets derived from the GOES 8 data are reasonable given the amount of drizzle in this two-layer cloud system. The drizzle is evident in the radar image of the clouds over the central facility in Plate 1. Some minor drizzle occurred around 1507 UTC but was not consistent until 1600 UTC. After 1700 UTC it did not reach the surface until 1750 UTC. The drizzle tapered off after 1800 UTC before a light rain began around 1940 UTC. The Egrett and Twin Otter data were analyzed for the period between 1700 and 1930 UTC. It is clear from Plate 1 that the cloud system observed during the October 30 flights was not a simple plane parallel cloud but a rather complex and variable two-layer system with imbedded precipitation cells.

7.3. October 13

Other days of special interest are those when cloud cover varied during the flight because such circumstance allows observation of the different conditions with the same untouched instruments. For example, *Cess et al.* [1999] analyzed the October 13 flight that started as a clear day, became increasingly cloudy, and finally became overcast in the afternoon. They showed that acceptance of the standard model prediction of cloudy-sky absorption would require that the bias error in the measurements of upwelling fluxes at the Egrett altitude change from essentially zero for the clear sky to -150 Wm^{-2} for the overcast sky. The present results also necessitate the same bias behavior to occur during the mixed conditions prevailing on September 25 and November 1. Furthermore, because of the agreement between GOES 8 and TSBR (Figure 9), the GOES 8 albedos would have to suffer the same change in bias error simultaneously. The likelihood of this type of bias behavior occurring simultaneously for instruments on such different platforms is very low, and such a change is incompatible with the observed stability of the GOES 8 visible channel and the RAMS instruments.

7.4. Possible Bias in GOES 8 Albedos

Li et al. [1998] found that the albedo-transmittance slope derived from GOES 7 data and ARM surface radiometer measurements during April 1994 showed better agreement with model calculations than the results in Figure 16. They attributed the differences between models and measurements to calibration errors in the GOES 8 data set. The evidence provided earlier, however, indicates that the calibration of the GOES 8 visible channel is accurate and stable. Furthermore, the comparison of the GOES 8 broadband albedos with broadband measurements from three different sources over 4 years of data provides ample evidence that the GOES 8 data are not the source of the GOES 7/GOES 8 slope difference. Other factors are required to explain the differences. The ARM surface radiometer calibrations were changed on October 1995 to conform to the April 1996 comparisons with World Radiation Reference standards [*Michalsky et al.*, 1997; *Kato et al.*, 1997]. However, even the adjustment in calibrations still leave undetermined the uncertainties introduced by thermal effects on the CART site pyranometers [*Bush et al.*, 1999b; *Cess et al.*, submitted manuscript, 1999].

8. Summary and Conclusions

Data sets acquired during ARESE from five independent experimental platforms (i.e., GOES 8, surface, and three aircraft) are checked for consistency, combined, and analyzed to test the ability of model calculations to predict the amount of solar radiation absorbed by the atmosphere. The consistency between aircraft, surface, and satellite instruments, together with the side-by-side (wing-to-wing) comparisons of instruments and the comparison of downwelling fluxes at 13 km altitude with model calculations (Pope and Valero, submitted manuscript, 1999), points to an accurate multiplatform data set covering 4 days during ARESE. This data set was analyzed to determine the absorption of solar radiation by the clear and cloudy atmospheres.

Broadband solar albedos deduced from GOES 8 are compared to ER 2, Egrett, and Twin Otter albedos and found to show stability and agreement well within the uncertainties in all cases during ARESE, except for days when aircraft anom-

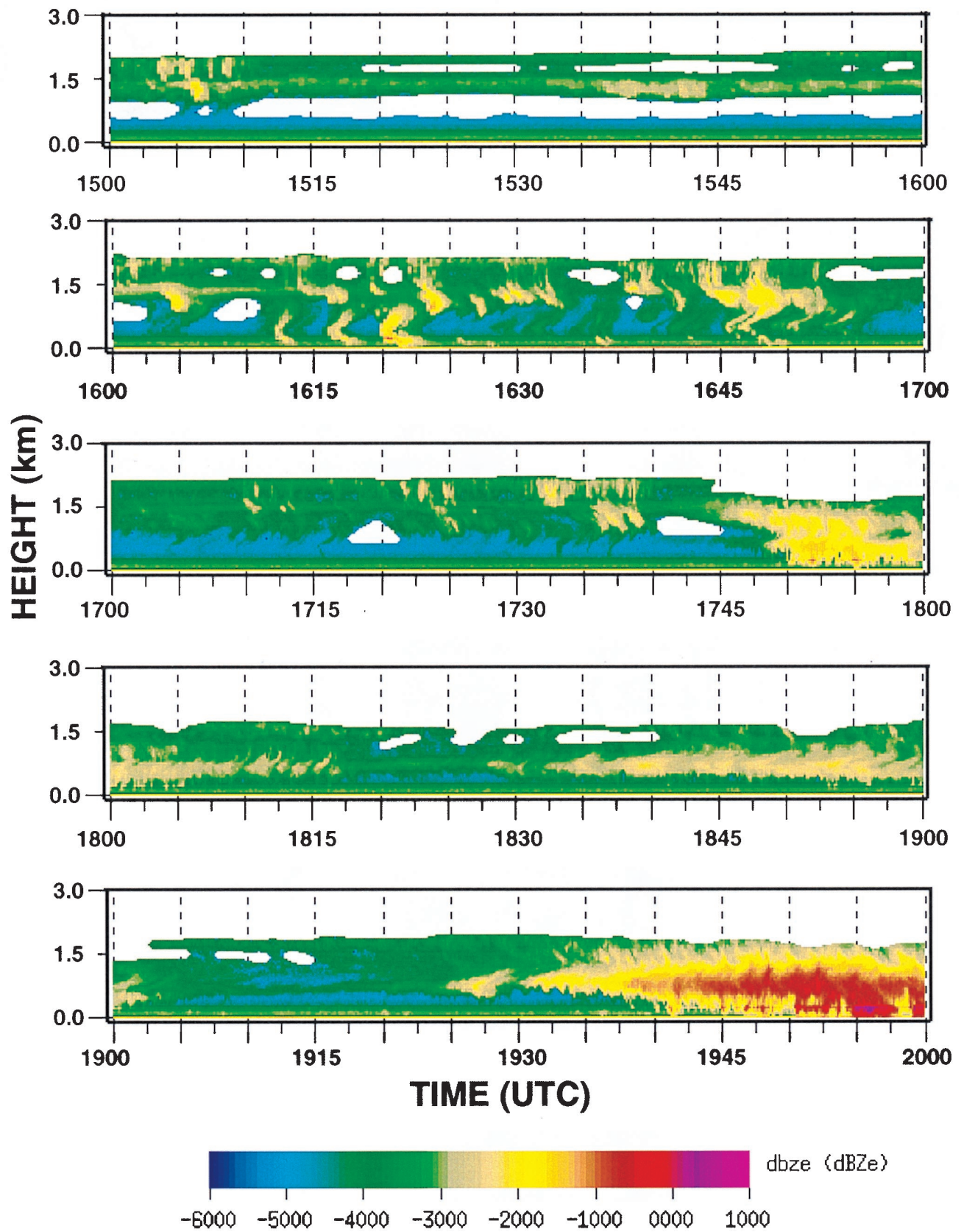


Plate 1. Radar reflectivity profiles from Pennsylvania State University 94 GHz cloud radar at ARM Central Facility during October 30, 1995.

alies in the Egrett are suspected. The flux divergence and TOA albedo versus surface transmittance analyses using aircraft, satellite, and surface data provide strong evidence for excess absorption by the cloudy atmosphere when compared to model estimates. For heavy overcast conditions the absorptance of solar radiation by the column between 0.5 and 13 km is 0.32 ± 0.03 , as determined from the aircraft measurements, while the GOES 8 albedo versus surface transmittance analysis gives an absorptance of 0.33 ± 0.04 for the total atmosphere (surface to top). The results for September 25, October 11, October 13, and November 1 indicate a cloudy-sky absorptance of 0.08 ± 0.06 in the visible spectral range (0.224–0.68 μm). Reexamination of previous results for October 30 yields a total solar absorptance of 0.31 ± 0.04 and an ultraviolet-visible absorptance of 0.04 ± 0.06 . The relatively large uncertainties in the “visible” absorptances make it difficult to assign their true magnitude and origin. The 500 nm absorptances that were reported by Valero *et al.* [1997a] suggest that at least part of the observed ultraviolet-visible absorptance may result from aerosols.

The differences in albedo, cloud optical depth, and particle sizes retrieved from GOES 8 and from surface data are shown to be consistent with excess absorption. The source of the excess absorption is still elusive, but the results presented here eliminate observational uncertainties as the primary cause of the measurement-modeling discrepancy.

Appendix: Relationship Between Transmittance, Absorptance, and Reflectance of an Atmospheric Layer and the Albedo Below the Layer

The absorption a by an atmospheric layer between altitudes U and L is defined as (see Figure 18):

$$a = F_U^+ - F_U^- - (F_L^+ - F_L^-)$$

and substituting $F_L^- = \alpha F_L^+$ yields

$$\begin{aligned} a &= F_U^+ - F_U^- - (F_L^+ - \alpha F_L^+) \\ &= F_U^+ - F_U^- - [(1 - \alpha) F_L^+], \end{aligned} \quad (2)$$

where F_U^+ and F_U^- are the downwelling and upwelling irradiances at the upper level, F_L^+ and F_L^- are the downwelling and upwelling irradiances at the lower level, and α is the albedo of the surface plus the layer below altitude L . Dividing (2) by F_U^+ ,

we obtain, in terms of absorptance ($A_{\text{layer}} = a/F_U^+$), reflectance ($R_{\text{layer} + \text{surface}} = F_U^-/F_U^+$), and transmittance ($T_{\text{layer}} = F_L^+/F_U^+$), where layer refers to layer quantities and $R_{\text{layer} + \text{surface}}$ is the reflectance of the layer plus the atmosphere and surface below the layer:

$$A_{\text{layer}} = 1 - R_{\text{layer} + \text{surface}} - (1 - \alpha)T_{\text{layer}},$$

which upon rearranging terms becomes

$$A_{\text{layer}} + R_{\text{layer} + \text{surface}} + T_{\text{layer}} = 1 + \alpha T_{\text{layer}}. \quad (3)$$

Equation (3) applies to the general case for which $\alpha \neq 0$ and $T_{\text{layer}} \neq 0$.

A case of particular interest, commonly observed over land and ice surfaces, occurs when $A_{\text{layer}} \leq \alpha T_{\text{layer}}$, resulting in

$$R_{\text{layer} + \text{surface}} + T_{\text{layer}} \geq 1. \quad (4)$$

For $\alpha = 0$ the reflectance term $R_{\text{layer} + \text{surface}}$ becomes R_{layer} , and (3) gives

$$A_{\text{layer}} + R_{\text{layer}} + T_{\text{layer}} = 1, \quad (5)$$

which is the textbook case for an idealized isolated column with no reflecting surface below (no energy entering the column from below).

Acknowledgments. ARESE was conducted under the auspices of the Department of Energy’s Atmospheric Radiation Measurements Program (ARM) and its Unmanned Aerospace Vehicle (UAV) component. NASA supported the deployment of the ER 2 aircraft. The innumerable contributions of the multilaboratory field team that organized and managed the field deployment are gratefully acknowledged. Discussions with members of the ARESE science team resulted in important contributions to the experimental and data analysis components of the project. Discussions with R. D. Cess were most helpful. We also want to thank very specially the anonymous reviewers for their major contributions, which improved the presentation of our results. This research was partially supported by the Department of Energy grant DEFG0395ER69183 to the Scripps Institution of Oceanography and NASA grant NAG 1-2044 to the Atmospheric Research Laboratory, Scripps Institution of Oceanography, University of California, San Diego. The satellite analyses were supported by the Department of Energy Environmental Sciences Division Interagency Agreement DE-AI02-97ER62341 as part of the Atmospheric Radiation Measurement Program. The radar imagery was obtained from the Pennsylvania State University World Wide Web site <http://www.arc.essc.psu.edu/data/index.html>.

References

- Arking, A., Absorption of solar energy in the atmosphere: Discrepancy between model and observations, *Science*, 273, 779–782, 1996.
- Arking, A., Bringing climate models into agreement with observations of atmospheric absorption, *J. Clim.*, 12, 1589–1600, 1999.
- Ayers, J. K., L. Nguyen, W. L. Smith Jr., and P. Minnis, Calibration of geostationary satellite imager data for ARM using AVHRR and VIRS, paper presented at 8th Annual ARM Science Team Meeting, Dep. of Energy, Tucson, Ariz., March 23–27, 1998.
- Bener, P., Untersuchung über die Wirkungsweise des Solarigraphen Moll-Gorczyński: Beiträge zur Strahlungsmethodik III, *Arch. Meteorol. Geophys. Bioklimatol., Ser. B*, 2, 188–249, 1950.
- Bush, B. C., and F. P. J. Valero, Comparison of ARESE clear sky surface radiation measurements, *J. Quant. Spectrosc. Radiat. Transfer*, 61, 249–264, 1999.
- Bush, B. C., S. K. Pope, A. Bucholtz, F. P. J. Valero, and A. Strawa, Surface radiation measurements during the ARESE campaign, *J. Quant. Spectrosc. Radiat. Transfer*, 61, 237–247, 1999a.
- Bush, B. C., F. P. J. Valero, A. S. Simpson, and L. Bignone, Characterization of thermal effects in pyranometers: A data correction algorithm for improved measurements of surface insolation, *J. Atmos. Oceanic Technol.*, in press, 1999b.

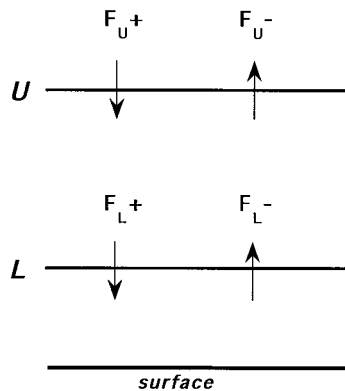


Figure 18. Schematic to illustrate the transmittance, absorptance, and reflectance of an atmospheric layer as discussed in the appendix.

- Cess, R. D., et al., Absorption of solar radiation by clouds: Observations versus models, *Science*, 267, 496–499, 1995.
- Cess, R. D., M. Zhang, F. P. J. Valero, S. K. Pope, A. Bucholtz, B. Bush, C. S. Zender, and J. Vitko Jr., Absorption of solar radiation by the cloudy atmosphere: Further interpretations of collocated aircraft measurements, *J. Geophys. Res.*, 104, 2059–2066, 1999.
- Charlock, T. P., and T. L. Alberta, The CERES/ARM/GEWEX Experiment (CAGEX) for the retrieval of radiative fluxes with satellite data, *Bull. Am. Meteorol. Soc.*, 77, 2673–2683, 1996.
- Charlock, T., F. R. Rose, T. L. Alberta, and G. D. Considine, Comparison of computed and measured cloudy-sky SW in ARESE, paper presented at 8th Annual ARM Science Team Meeting, Dep. of Energy, Tucson, Ariz., March 23–27, 1998.
- Collins, W. D., A global signature of enhanced shortwave absorption by clouds, *J. Geophys. Res.*, 103, 31,669–31,679, 1998.
- Crisp, D., Absorption of sunlight by water vapor in cloud conditions: A partial explanation for the cloud absorption anomaly, *Geophys. Res. Lett.*, 24, 571–574, 1997.
- Doelling, D. R., W. L. Smith Jr., T. L. Alberta, J. K. Ayers, P. Minnis, F. P. J. Valero, and S. Pope, An examination of shortwave albedos determined from narrowband visible radiances using ARM/UAV data, paper presented at AMS Ninth Conference on Atmospheric Radiation, Am. Meteorol. Soc., Long Beach, Calif., Feb. 2–7, 1997.
- Doelling, D. R., L. Nguyen, W. L. Smith Jr., and P. Minnis, Comparison of ARM GOES-derived broadband fluxes and albedos with broadband data from ARM-UAV, ScaRaB, and CERES, paper presented at 8th Annual ARM Science Team Meeting, Dep. of Energy, Tucson, Ariz., March 23–27, 1998.
- Doelling, D. R., W. L. Smith Jr., P. Minnis, and F. P. J. Valero, Broadband radiation fluxes from narrowband radiances, paper presented at ALPS 99 Conference, Cent. Natl. d'Etudes Spatiales, Meribel, France, January 18–22, 1999.
- Dong, X., T. P. Ackerman, E. E. Clothiaux, P. Pilewskie, and Y. Han, Microphysical and radiative properties of stratiform clouds deduced from ground-based measurements, *J. Geophys. Res.*, 102, 23,829–23,843, 1997.
- Drummond, K. L., and J. J. Roche, Corrections to be applied to measurements made with Eppley (and other) spectral radiometers when used with Schott colored glass filters, *J. Appl. Meteorol.*, 4, 741–744, 1965.
- Francis, P., J. Taylor, P. Hignett, and A. Slingo, On the question of enhanced absorption of solar radiation by clouds, *Q. J. R. Meteorol. Soc.*, 123, 419–434, 1997.
- Fritz, S., Solar radiant energy, in *Compendium of Meteorology*, edited by T. F. Malone, pp. 14–29, John Wiley, New York, 1951.
- Fu, Q., and K.-N. Liou, Parameterization of the radiative properties of cirrus clouds, *J. Atmos. Sci.*, 49, 2139–2136, 1993.
- Gulbrandsen, A., On the use of pyranometers in the study of spectral solar radiation and atmospheric aerosols, *J. Appl. Meteorol.*, 17, 899–904, 1978.
- Halothore, R., S. Nemesure, S. Schwartz, D. Imre, A. Berk, E. Dutton, and M. Bergin, Models overestimate diffuse clear-sky surface irradiance: A case for excess atmospheric absorption, *Geophys. Res. Lett.*, 25, 3591–3594, 1998.
- Hammer, P. D., F. P. J. Valero, and S. Kinne, The 27–28 October 1986 FIRE cirrus case study: Retrieval of cloud particle sizes and optical depths from comparative analyses of aircraft and satellite-based infrared measurements, *Mon. Weather Rev.*, 119, 1673–1692, 1991.
- Hayasaka, T., T. Nakajima, Y. Fujiyoshi, Y. Ishikawa, T. Takeda, and M. Tanaka, Geometrical thickness, liquid water content, and radiative properties of stratocumulus clouds over the western North Pacific, *J. Appl. Meteorol.*, 34, 460–470, 1995a.
- Hayasaka, T., N. Kikuchi, and M. Tanaka, Absorption of solar radiation by stratocumulus clouds: Aircraft measurements and theoretical calculations, *J. Appl. Meteorol.*, 34, 1047–1055, 1995b.
- Imre, D., E. Abramson, and P. Daum, Quantifying cloud-induced short-wave absorption: An examination of uncertainties and of recent arguments for large excess absorption, *J. Appl. Meteorol.*, 35, 1991–2010, 1996.
- Kato, S., T. Ackerman, E. Clothiaux, J. Mather, G. Mace, M. Wesely, F. Murcray, and J. Michalsky, Uncertainties in modeled and measured clear-sky surface short-wave irradiances, *J. Geophys. Res.*, 102, 25,881–25,898, 1997.
- Kiehl, J. T., J. J. Hack, M. H. Zhang, and R. D. Cess, Sensitivity of a GCM climate to enhanced shortwave cloud absorption, *J. Clim.*, 8, 2200–2212, 1995.
- Li, Z., and L. Moreau, Alteration of atmospheric absorption by clouds: Simulation and observation, *J. Appl. Meteorol.*, 35, 653–670, 1996.
- Li, Z., L. Moreau, and A. Arking, On solar energy disposition: A perspective from observation and modeling, *Bull. Am. Meteorol. Soc.*, 78, 53–70, 1997.
- Li, Z., A. Trishchenko, H. W. Barker, G. L. Stephens, P. Partain, and P. Minnis, Consistency analyses of ARESE measurements for studying cloud absorption, paper presented at 8th Annual ARM Science Team Meeting, Dep. of Energy, Tucson, Ariz., March 23–27, 1998.
- Lin, B., and P. Minnis, Temporal variations of land surface microwave emissivities over the ARM Southern Great Plains site, *J. Appl. Meteorol.*, in press, 1999.
- Loeb, N., In-flight calibration of NOAA AVHRR visible and near-IR bands over Greenland and Antarctica, *Int. J. Remote Sens.*, 18, 477–490, 1997.
- Lubin, D., and A. S. Simpson, Measurement of surface radiation fluxes and cloud optical properties during the 1994 Arctic Ocean Section, *J. Geophys. Res.*, 102, 4275–4286, 1997.
- Marshak, M. A., A. Davis, W. Wiscombe, and R. Cahalan, Inhomogeneity effects on cloud short-wave absorption measurements: Two-aircraft simulations, *J. Geophys. Res.*, 102, 16,619–16,637, 1997.
- Michalsky, J., M. Rubes, T. Stoffel, M. Wesely, M. Splitt, and J. DeLuisi, Optimal measurements of surface shortwave irradiance using current instrumentation: The ARM experience, paper presented at AMS Ninth Conference on Atmospheric Radiation, Am. Meteorol. Soc., Long Beach, Calif., Feb. 2–7, 1997.
- Minnis, P., and W. L. Smith Jr., Cloud and radiative fields derived from GOES-8 during SUCCESS and the ARM-UAV Spring 1996 Flight Series, *Geophys. Res. Lett.*, 25, 1113–1116, 1998.
- Minnis, P., W. L. Smith Jr., D. P. Garber, J. K. Ayers, and D. R. Doelling, Cloud properties derived from GOES-7 for the Spring 1994 ARM Intensive Observing Period using Version 1.0.0 of the ARM satellite data analysis program, *NASA Republ.*, 1366, 59 pp., 1995a.
- Minnis, P., D. P. Kratz, J. A. Coakley Jr., M. D. King, D. Garber, P. Heck, S. Mayor, D. F. Young, and R. Arduini, Cloud optical property retrieval (subsystem 4.3), in *Clouds and the Earth's Radiant Energy System (CERES) algorithm theoretical basis document*, vol. III; *Cloud Analyses and Radiance Inversions (Subsystem 4)*, edited by CERES Science Team, *NASA Republ.*, 1376, 135–176, 1995b.
- Minnis, P., S. Mayor, W. L. Smith Jr., and D. F. Young, Asymmetry in the diurnal variation of surface albedo, *IEEE Trans. Geosci. Remote Sens.*, 35, 879–891, 1997.
- Minnis, P., D. P. Garber, D. F. Young, R. F. Arduini, and Y. Takano, Parameterization of reflectance and effective emittance for satellite remote sensing of cloud properties, *J. Atmos. Sci.*, 55, 3313–3339, 1998.
- Morikofer, W., Meteorologische Strahlungsmessmethoden, in *Handbuch der Biologischen Arbeitsmethoden*, edited by E. Abderhalden, pp. 4005–4245, Urban and Schwarzenberg, Berlin, 1939.
- Nguyen, L., P. Minnis, J. K. Ayers, W. L. Smith Jr., and S. P. Ho, Intercomparison of geostationary and polar satellite data using AVHRR, VIRS, and ATSR-2 data, paper presented at AMS 10th Conference on Atmospheric Radiation, Am. Meteorol. Soc., Madison, Wis., June 28 to July 2, 1999.
- Partain, P., S. Miller, R. F. McCoy, G. L. Stephens, and P. M. Gabriel, Testing radiation models using spectral fluxes and radiances measured from aircraft, paper presented at 8th Annual ARM Science Team Meeting, Dep. of Energy, Tucson, Ariz., March 23–27, 1998.
- Pilewskie, P., and F. P. J. Valero, Direct observations of excess solar absorption by clouds, *Science*, 267, 1626–1629, 1995.
- Pilewskie, P., and F. P. J. Valero, Response to “How much solar radiation do clouds absorb?”, *Science*, 271, 1134–1136, 1996.
- Ramanathan, V., et al., Warm pool heat budget and short-wave cloud forcing: A missing physics?, *Science*, 267, 499–503, 1995.
- Robinson, N., *Solar Radiation*, pp. 247–271, Elsevier Sci., New York, 1966.
- Rodskjer, N., A pyranometer with dome of RG8 for use in plant communities, *Arch. Meteorol. Geophys. Bioklimatol, Ser. B19*, 307–320, 1971.
- Stamnes, K., S.-C. Tsay, W. J. Wiscombe, and K. Jayaweera, Numerically stable algorithm for discrete-ordinate-method radiative transfer in multiple scattering and emitting layered media, *Appl. Opt.*, 27, 2502–2509, 1988.
- Stephens, G. L., How much solar radiation do clouds absorb?, *Science*, 271, 1131–1133, 1996.

- Stephens, G. L., and S. C. Tsay, On the cloud absorption anomaly, *Q. J. R. Meteorol. Soc.*, *116*, 671–704, 1990.
- Stephens, G. L., R. F. McCoy, R. B. McCoy, P. Gabriel, P. T. Partain, and S. D. Miller, A multipurpose scanning spectrometer polarimeter (SSP): Instrument design and sample results, *J. Atmos. Oceanic Technol.*, in press, 1999.
- Valero, F. P., and B. C. Bush, Measured and calculated clear-sky solar radiative fluxes during the Subsonic Aircraft Contrail and Cloud Effects Special Study (SUCCESS), *J. Geophys. Res.*, *104*, 27,387–27,398, 1999.
- Valero, F. P. J., R. D. Cess, M. Zhang, S. K. Pope, A. Bucholtz, B. Bush, and J. Vitko Jr., Absorption of solar radiation by clouds: Interpretations of collocated aircraft measurements, *J. Geophys. Res.*, *102*, 29,917–29,927, 1997a.
- Valero, F. P. J., A. Bucholtz, B. C. Bush, S. K. Pope, W. D. Collins, P. Flatau, A. Strawa, and W. J. Y. Gore, Atmospheric radiation measurements enhanced short-wave experiment (ARESE): Experimental and data details, *J. Geophys. Res.*, *102*, 29,929–29,937, 1997b.
- Wielicki, B. A., et al., Clouds and the Earth's Radiant Energy System (CERES): Algorithm overview, *IEEE Trans. Geosci. Remote Sens.*, *36*, 1127–1141, 1998.
- Wild, M., A. Ohmura, H. Gilgen, and E. Roeckner, Validation of general circulation model radiative fluxes using surface observations, *J. Clim.*, *8*, 1309–1324, 1995.
- Wiscombe, W. J., A. Marshak, L. Oreopoulos, R. F. Cahalan, and A. B. Davis, Two methods for removing the effect of horizontal fluxes from stacked aircraft measurements of shortwave absorption by clouds, paper presented at 8th Annual ARM Science Team Meeting, Dep. of Energy, Tucson, Ariz., March 23–27, 1998.
- Zender, C. S., S. K. Pope, B. Bush, A. Bucholtz, W. D. Collins, J. T. Kiehl, and F. P. J. Valero, Atmospheric absorption during ARESE, *J. Geophys. Res.*, *102*, 29,901–29,927, 1997.
-
- A. Bucholtz, B. C. Bush, S. K. Pope, and F. P. J. Valero, Atmospheric Research Laboratory, Center for Atmospheric Sciences, Scripps Institution of Oceanography, University of California, San Diego, 9500 Gilman Drive, La Jolla, CA 92093-0242. (fvalero@ucsd.edu)
- D. R. Doelling, X. Dong, and W. L. Smith Jr., AS&M, Inc., Hampton, VA 23666.
- P. Minnis, Atmospheric Sciences Division, NASA Langley Research Center, Hampton, VA 23681.

(Received April 21, 1999; revised September 29, 1999; accepted October 5, 1999.)